

STUDY ON MECHANICAL CHARACTERISTICS OF GLASS FIBER-REINFORCED POLYCARBONATE LFT-D FOR CODICO STRUCTURES

Christoph Schelleis^{1,2}, Benedikt M. Scheuring³, Andrew Hrymak⁴ and Frank Henning^{1,2}

¹ Polymer Engineering, Fraunhofer Institute for Chemical Technology, Pfaffzettel, Germany, corresponding: christoph.schelleis@ict.fraunhofer.de, https://www.ict.fraunhofer.de/en/comp/polymer_engineering.html

² Institute of Vehicle Systems Technology, Karlsruhe Institute of Technology, Karlsruhe, Germany, <https://www.fast.kit.edu/english/lbt/index.php>

³ Institute for Applied Materials, Karlsruhe Institute of Technology, Karlsruhe, Germany, <https://www.iam.kit.edu/english/index.php>

⁴ Chemical and Biochemical Engineering, Western University, London, Canada, <https://www.eng.uwo.ca/chemical/index.html>

Keywords: Composite, Fiber length distribution, Fiber mass distribution, Tensile properties, Plastificate

ABSTRACT

Long fiber thermoplastic (LFT) materials can be compounded in an effective LFT direct (LFT-D) process. Polycarbonate (PC) is used in various applications for example in and around battery enclosures for electro mobility. Reinforced with glass fibers (GF), PC exhibits solid mechanical properties and is a promising and novel addition to the material portfolio of the LFT-D process considering current industry demands. Combining continuous (Co) and discontinuous (DiCo) fiber reinforced polymers (FRP) according to their respective strengths enables unique design freedom to this class of materials. LFT-D materials can be used as the DiCo phase. The semi-finished material of the LFT-D process, called plastificate, is placed in the charge area and will fill the mold during compression molding forming the flow area. These areas are very distinct in their microstructure.

In this work, PC GF LFT-D is produced at various process parameter sets and molded into plates. Screw speed and fiber roving amount is varied. Plates were characterized for their fiber mass fraction, fiber length and tensile properties. Fiber mass fraction as well as fiber length are very homogenous over charge and flow area. Tensile properties are characterized in the flow area in eight adjacent positions. A strong influence of sample position on modulus and strength, resulting in deviations of up to twenty-five percent from highest to lowest value, is present. Running the extruder at increasing screw speeds improves Young's modulus as well as tensile strength.

1 INTRODUCTION

Molding of continuous (Co) and discontinuous (DiCo) fiber reinforced materials has great lightweighting potential. Material is used where it is needed according to load paths, complex geometries, and other requirements. Various material systems across a wide variety of processes can be used for each of the phases [1]. Long fiber thermoplastic (LFT) materials offer a good compromise between mechanical performance and design freedom. LFT materials can be processed in various ways. One cost effective DiCo option is LFT-direct (LFT-D) processing demonstrated in various CoDiCo projects [7, 17, 18].

The process scheme of LFT-D compression molding is shown in Figure 1. Two twin screw extruders (TSEs) are used to compound the polymer matrix from granulate (TSE 1 also called ZSE) and to compound LFT-D from molten matrix material and continuous fiber rovings (TSE 2 also called ZSG). The resulting semi-finished material extruded from TSE 2 is called plastificate which is cut at specific lengths and subsequently compression molded. Plastificate geometry, especially the length is

determined by part geometry and thickness. The plastificate is the link between continuous extrusion and discontinuous compression molding. As such it has an old end and a new end. The “age” difference is usually shorter than the compression molding cycle time which depends on part size and thickness.

During compression molding the mold is filled and two microstructurally distinct areas are developed. Fiber orientation is dependent, among others, on extrusion direction and was described by various authors [20, 21, 23, 34]. The initial fiber orientation in the plastificate influences at least the mechanical characteristics in the charge area. Gandhi et al. have presented an overview of these investigations [9]. Mechanical properties overall are strongly dependent on fiber length and in the flow area by flow induced fiber orientation. The correlation of mechanical properties to fiber mass fraction and fiber length was shown by Thomason et al. for glass fiber (GF) reinforced polypropylene (PP) [31–33] as well as polyamide 6 (PA6) [27–30]. LFT materials change their fiber properties, length, and mass fraction, along the flow path. Gandhi et al. [9] as well as Rohde-Tibitz [25] present overviews of these phenomena for various processes including LFT-D. Changing fiber properties mean different mechanical properties.

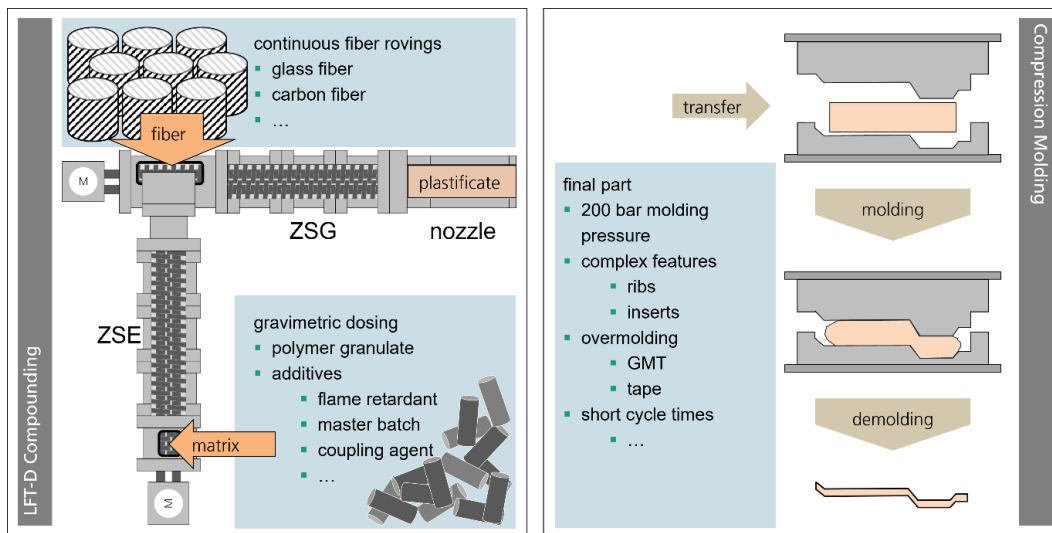


Figure 1: Processing scheme LFT-D compression molding. LFT-D compounding comprising two twin screw extruders is shown left. Shown right is the compression molding process [26].

Previous work in LFT-D was presented for PP [5, 14, 19, 22, 23, 34], PA 6 [15, 24, 37], PA 66 [2–4, 6] as well as specialty materials [8, 10–12, 26]. Where mechanical properties were investigated, the distinction is usually made between charge and flow area and the sampling is done accordingly. The work presented here expands upon a paper published by the authors dealing with process development for a novel LFT-D material system, polycarbonate (PC) GF. Detailed descriptions of parameter development are presented as well as a discussion of tensile and bending test results as well as impact properties. [26]

2 EXPERIMENTAL

The matrix material, PC Makrolon 2405, was provided by Covestro Deutschland AG. The GF material, StarRov 853, was provided by Johns Manville Europe GmbH. Trials were conducted on machines at Fraunhofer Institute of Chemical Technology. A Dieffenbacher LFT-D line comprising two 40 mm Leistritz TSEs and a Dieffenbacher parallel guided hydraulic press with a total press force of 5000 kN were used.

A selection of processing parameters, corresponding plates, additional tensile testing as well as additional fiber length measurements are discussed here. The following Table 1 shows these processing parameters. Fiber mass fraction is set to be 40 % for all parameter sets. The throughput of polymer

material was kept at 30 kg/h. Total LFT-D material throughput is at a constant 50 kg/h accordingly. This resulted in an age difference within the plastificate of around 45 s from oldest to newest material.

Plates of 400 mm² are molded at constant press closing profiles to a thickness of 4 mm with a press force of 3200 kN.

Table 1: Processing Parameters

Parameter set	Screw speed (rpm)	Roving amount (pcs)
V5	53	28
V7	62	24
V12	45	34
V16	36	41
V33	74	20

The fiber mass fraction was analyzed via thermogravimetric analysis (TGA). The samples were heated at 650°C for 12 hours. This removes the polymer matrix. During this process the samples are weighed, and the fiber mass fraction is calculated afterwards. Samples are taken for fiber length measurements.

Fiber length measurement is conducted via FASEP, an image evaluation method [13]. Ashed fiber residue from TGA is diluted in water following a controlled procedure. The water-fiber suspension is scanned, and the scans are evaluated for fiber lengths.

Tensile testing was conducted according to DIN EN ISO 527-5. Samples were taken from plates via water jet cutter in the locations 1 to 8 as indicated in Figure 2. The charge and flow area are designated here as well as extrusion direction and corresponding old and new end of the plastificate. To illustrate this scheme a top-down view of the plastificate in the mold before molding is shown on the upper right. On plates molded from LFT-D the charge area can be identified by characteristic rough surface appearance as can be seen on the lower right.

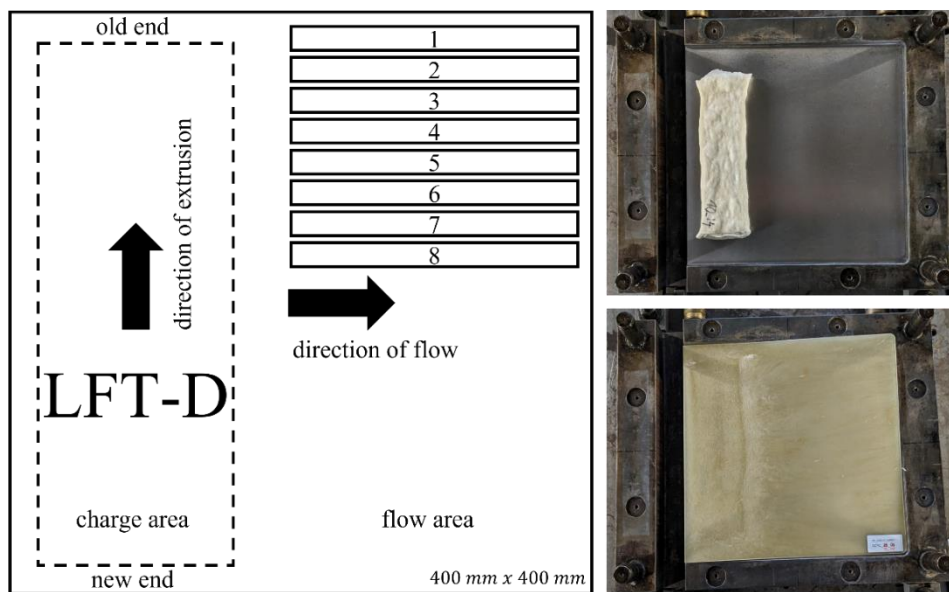


Figure 2: Distinct areas of an LFT-D plate shown schematically on the left. The charge area is where the plastificate is initially placed, upper right. During molding the flow area is formed, both areas are visually distinct as well (lower right).

3 RESULTS AND DISCUSSION

To describe the DiCo phase in CoDiCo, flow phenomena and resulting microstructures must be considered. When co-molding, additional restrictions on plastificate placement might have to be respected. These include secure positioning of Co-materials during mold filling and location of geometrical features. Fiber length and mass fraction can be considered representative of mechanical properties and are discussed here first.

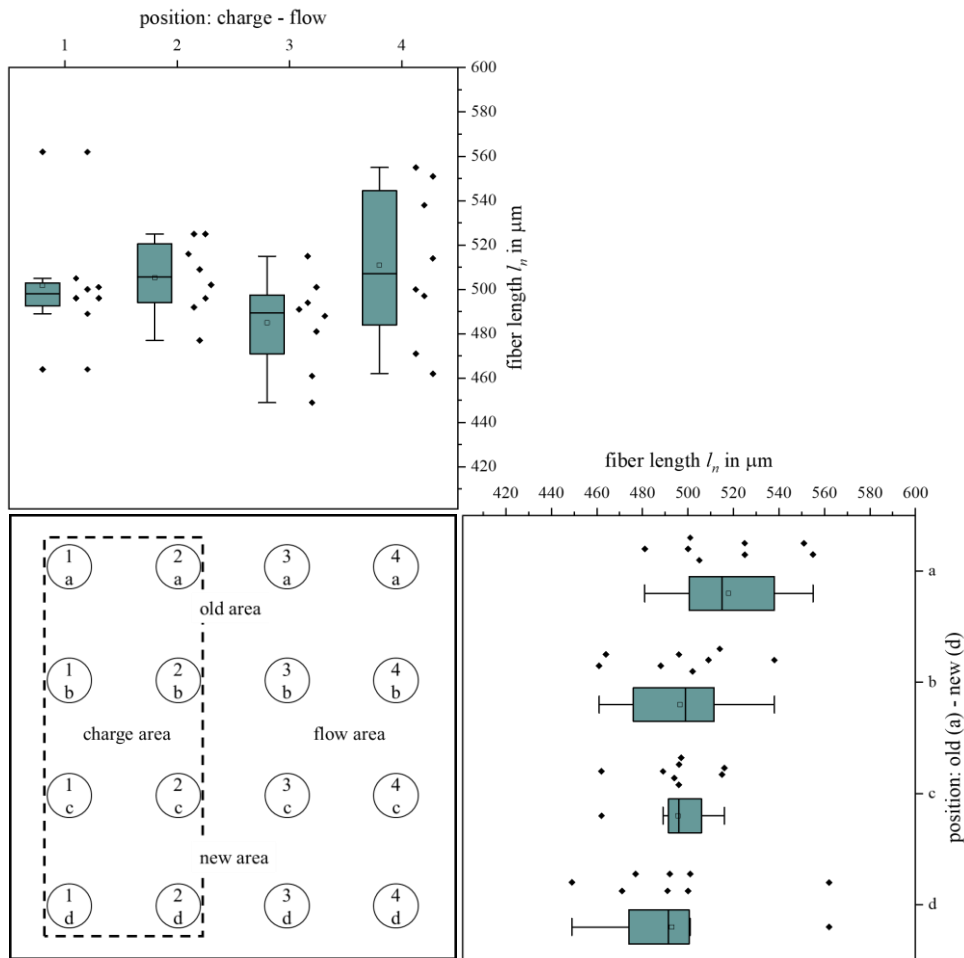


Figure 3: Number average fiber lengths l_n for two plates from parameter set V33 sorted by columns and rows representing the flow path (1 to 4 upper left) and plastificate age (a to d lower right). The sampling scheme is given in the lower left.

The fiber length distribution for two plates (400 mm by 400 mm) is shown in detail in Figure 3. The sampling scheme is shown in the lower left. The plastificate placement area is indicated by the dashed lines similar to Figure 2. A total of 16 samples per plate were taken in an equidistant four by four grid. All distances are 80 mm. Rows are indicated by letters a to d, columns are indicated by numbers 1 through 4. Both designations are also displayed on every sampling position. The standard box plots show four quartiles of the data set, the whiskers representing first and fourth quartile. The median is indicated by a black line in the box. The mean value for every row and column is indicated by a quadratic box symbol. All measured mean fiber lengths per sampling position are displayed as black dots next to the boxes, between eight to ten thousand individual fibers are measured for every position. Two outliers exist in samples 1c and 1d. They are displayed in line of the whiskers of the box plots of column 1 and row c and d.

Columns 1 and 2 can be assigned to the charge area and columns 3 and 4 represent the flow area. The spread of fiber lengths increases with flow length from column 1 to column 4. Median and mean values are all at around 500 μm . The following statements can be made on PC GF LFT-D:

1. Fiber lengths in PC GF LFT-D do not differ over wide parameter variations [26].
2. Fiber lengths are equally not affected by the flow during mold filling. Fiber shortening does not happen.

Fiber lengths are also evaluated by row in the box plot on the lower right. The age of the plastificate has been sectioned from old (a) to new (d). The spread as well as the mean value increases slightly, again insignificantly, towards the old end (a).

Evaluating the data in other ways, by grouping the sampling positions, for example as quarters or sixteenths does not yield further findings. Fiber lengths are often weight averaged to account for the increased impact of longer fibers on the mechanical properties. The weight average fiber length l_w calculated from 32 measurements for these sampled plates is 1254 μm and does also not differ significantly over either flow path or age.

The same type of plot can be arranged for fiber mass fraction. Results of fiber mass fraction measurements via TGA are shown in Figure 4. The sampling scheme shown in Figure 3, bottom left, was omitted here due to redundancy. The positions of x- and y- axis have been retained for the sake of consistency.

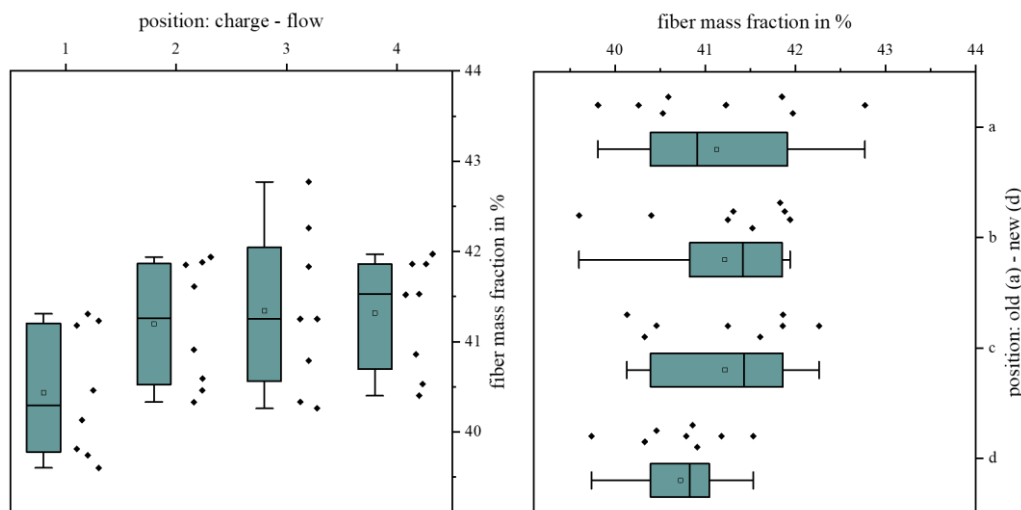


Figure 4: Fiber mass fraction for two sample plates from parameter set V33 sorted by columns and rows representing the flow path (1 to 4 on the left) and plastificate age (a to d on the right).

Targeted fiber mass fractions for all trials were 40 %. Overall, the measured fiber mass fraction at 41.07 % is higher than it was set to be. This is because the continuous fibers are drawn into the second TSE as a function of screw speed and roving amount. This is subject to slippage depending on screw speed which can only be corrected by empirically measuring a fiber intake factor which was not available for this material combination. A detailed explanation regarding the fiber intake factor is given by Schelleis et al. [26] and was mentioned before by Tröster [34] as well as Truckenmüller [35, 36] among others. The mean fiber mass fraction increases slightly from 40.4 % to 41.3 % along the flow length. The spread of measured values increases with plastificate age (from d to a). None of the effects are significant. One further statement can be added to the previous list:

3. Fiber-matrix separation as described in the state of the art and observed in LFT-D compression molding for other material systems like PP or PA does not occur for PC.

Having established that neither fiber mass fraction nor fiber length do significantly differ on a sample plate, tensile properties of eight samples taken in 0° orientation from the old, flow area are now

discussed. Refer to Figure 2, left part, for these sampling positions 1 through 8. Remaining in the designation scheme from Figure 3 and Figure 4, the intersection between columns 3 and 4 and rows a and b is sampled here. In the following Figure 5 young's modulus in GPa over said positions is shown. A selection of processing parameters is shown for reference on top of the figure.

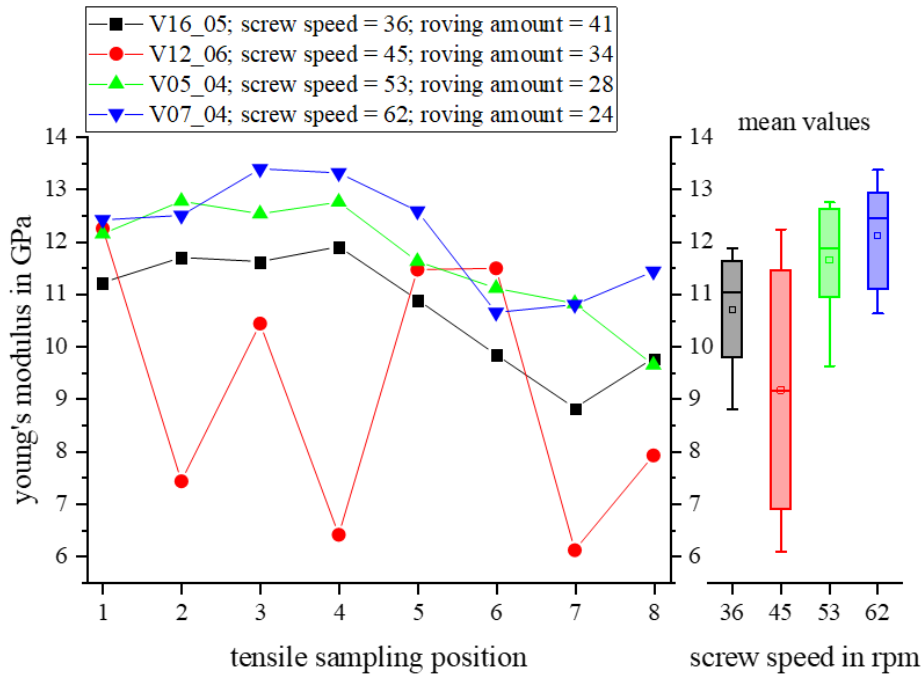


Figure 5: Young's modulus over eight sampling positions from the old flow area in 0° direction (left). Box plots of results per parameter set sorted by ascending screw speed(right).

A characteristic curve can be identified for sampling series V5, V7 and V16. Young's modulus is increasing from position 1 through 4 then decreases to position 6 and levels out through to position 8. It is unclear why testing of parameter set V12 returned unsteady results that could also not be explained after visual inspection of the tested specimens.

Mean values calculated over all samples are displayed in a box plot on the right. The results are arranged according to screw speed. While statistically insignificant, a slight increase in mean young's modulus towards higher screw speeds can be seen from 10.7 GPa to 12.1 GPa. This may correspond to slightly higher fiber lengths reported for higher screw speeds [26]. Higher screw speeds generally generate higher shear forces that result in better fiber dispersion and impregnation [16].

In the following Figure 6, tensile strengths are shown in similar fashion. The same overall decline in properties towards the middle line of the plate can be observed as before. Again, before declining, the tensile strength reaches a maximum between sample position 2 and 4. Plotting box plots for all eight samples shown on the right of the figure shows again a slight increase of properties towards higher screw speeds.

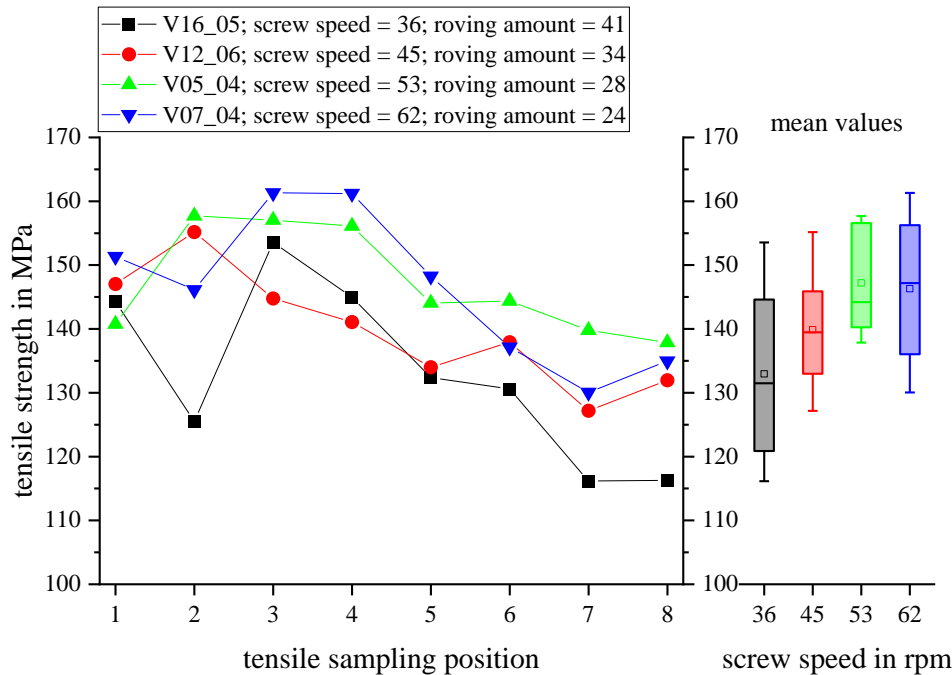


Figure 6: Tensile strength over eight sampling positions from the old flow area in 0° direction (left). Box plots of results per parameter set sorted by ascending screw speed(right).

The difference between sampling positions, for example from 3 and 4 to 7 and 8, is significant. While it is normal for LFT-D characteristics to scatter due to possible fiber agglomerations etc. it is noteworthy that the increase and decrease in mechanical properties follows a very similar curve for various parameter sets. Even considering the closeness of sample 1 and 2 to the mold edge, where fiber orientation might be affected, the remaining decline in properties is still around 20-25 % from highest to lowest value.

Again, the tensile strength increases with screw speed from a mean value of 133 MPa at 36 rpm to 146 MPa at 62 rpm.

The plastificate does not perfectly match the entire length of the mold, so material flow especially towards the mold edges might be affected and fiber orientation not ideally oriented in 0° to the flow direction. This was noted by Tröster who described a shift in main fiber orientation in plates of around 10° out of the 0° flow direction [34]. Radkte [23] explored these phenomena further and added, that plastificate temperature from old to new end increases by 20 K, suggesting that material viscosity might influence material flow additionally to the observations Tröster made [34]. Bondy and Altenhof noticed in their work on carbon fiber reinforced PA6 LFT-D, that samples taken from 45° direction exhibited better properties than similar samples from -45° direction, hinting towards the same phenomenon [2].

4 CONCLUSIONS

PC GF40 LFT-D was processed and sampled regarding fiber and tensile properties for various parameter sets.

Neither fiber matrix separation nor fiber length shortening occurs over the flow path or plastificate age as was shown in Figure 3 and Figure 4. PC GF presents a very homogenous LFT-D core material for CoDiCo structures.

A significant change of properties over sampling positions can be seen for tensile testing. This is in good agreement with studies conducted in the past. In the future, cutting schemes for sampling need to consider that a lot of scatter will result from sample placement. It is encouraged to cut more plates on the same position than to sample one plate in more positions.

Detailed investigations into how plasticate properties, geometry, or temperature, influence the characterization next to known factors like fiber length, mass and initial orientation shall be done to improve parameter optimization.

ACKNOWLEDGEMENTS

The research documented in this manuscript has been funded by the Deutsche Forschungsgemeinschaft (DFG, German Research Foundation), project number 255730231, within the International Research Training Group “Integrated engineering of continuous-discontinuous long fiber reinforced polymer structures “(GRK 2078). The support by the German Research Foundation (DFG) is gratefully acknowledged. Support from Covestro Deutschland AG as well as Johns Manville Europe GmbH in form of trial materials is gratefully acknowledged.

REFERENCES

- [1] Böhlke, T., Henning, F., Hrymak, A., Kärger, L., Weidenmann, K., and Wood, J. T., Eds. 2019. *Continuous--discontinuous fiber-reinforced polymers. An integrated engineering approach*. Carl Hanser Verlag, Munich.
- [2] Bondy, M. and Altenhof, W. 2020. Experimental characterisation of the mechanical properties of a carbon fibre/PA66 LFT automotive seatback under quasi-static and impact loading. *International Journal of Crashworthiness* 25, 4, 401–420.
- [3] Bondy, M., Mohammadkhani, P., Magliaro, J., and Altenhof, W. 2022. Elevated Strain Rate Characterization of Compression Molded Direct/In-Line Compounded Carbon Fibre/Polyamide 66 Long Fibre Thermoplastic. *Materials (Basel, Switzerland)* 15, 21.
- [4] Bondy, M., Pinter, P., and Altenhof, W. 2017. Experimental characterization and modelling of the elastic properties of direct compounded compression molded carbon fibre/polyamide 6 long fibre thermoplastic. *Materials & Design* 122, 184–196.
- [5] Buck, F., Brylka, B., Müller, V., Müller, T., Weidenmann, K. A., Hrymak, A. N., Henning, F., and Böhlke, T. 2015. Two-scale structural mechanical modeling of long fiber reinforced thermoplastics. *Composites Science and Technology* 117, 1, 159–167.
- [6] Dahl, J. S., Blanchard, P. J., and Rodgers, W. R. 2012. Direct compounding of a carbon fiber reinforced polyamide 66 composite. In *Technical Conference Proceedings*.
- [7] Deinzer, G., Kothmann, M., Rausch, J., Baumgärtner, S., Rosenberg, P., Link, T., Diebold, F., Roquette, D., and Henning, F. 2017. Research Project SMiLE – Manufacturing Technologies for continuous fibre-reinforced lightweight automotive floor modules for cost-efficient high volume production. In *SAMPE Europe Conference*.
- [8] Eyerer, P., Krause, W., Geiger, O., and Henning, F. 2006. Development of a Technology for the Large-Scale Production of Continuous Fiber Reinforced Composites. *SPE Annual Technical Conference ANTEC*.
- [9] Gandhi, U. N., Goris, S., Osswald, T. A., and Song, Y.-Y. 2020. *Discontinuous fiber-reinforced composites. Fundamentals and applications*. Hanser Publishers, München, Germany.
- [10] Geiger, O., Eyerer, P., Henning, F., and Brüssel, R. 2005. Back-Molding of High-Gloss Films with Long Fiber-Reinforced Thermoplastics. *ANTEC Society of Plastics Engineers SPE 2005*, 63, 2792–2796.
- [11] Geiger, O., Henning, F., Eyerer, P., Brüssel, R., and Ernst, H. 2006. LFT-D: materials tailored for new applications. *Reinforced Plastics* 50, 1, 30–35.
- [12] Geiger, O., Seib, W., and Brüssel, R. 2004. Folientechnologie für die Herstellung großflächiger Class-A Außenhautbauteile aus langfaserverstärkten Thermoplasten.
- [13] Hartwich, M. R., Höhn, N., Mayr, H., Sandau, K., and Stengler, R. 2009. FASEP ultra-automated analysis of fibre length distribution in glass-fibre-reinforced products. In *Optical Measurement Systems for Industrial Inspection VI*. SPIE Proceedings. SPIE, 738921. DOI=10.1117/12.827503.
- [14] Henning, F. 2001. *Verfahrensentwicklung für lang- und endlosglasfaserverstärkte thermoplastische Sandwich-Bauteile mit geschlossenem Werkstoff-Kreislauf*. Wissenschaftliche Schriftenreihe des Fraunhofer ICT Bd. 34. Fraunhofer-IRB-Verl., Stuttgart, Germany.

- [15] Huembert, S. 2016. *MA Influence of the screw configuration on the LFT-D processing of glass fiber reinforced PA6.*
- [16] Kohlgrüber, K. 2020. *Co-Rotating Twin-Screw Extruders - Two Volume Set.* Carl Hanser Verlag GmbH & Co. KG, München.
- [17] Link, T., Baumgärtner, S., Dörr, D., and Henning, F. 2018. Hybrid thermoplastic composites for automotive applications - development and manufacture of a lightweight rear floor structure in multi-material design. In *Materials Science: Fiber-Hybrid Composites.*
- [18] Link, T., Behnisch, F., Rosenberg, P., Seuffert, J., Dörr, D., Hohberg, M., Joppich, T., and Henning, F. 2019. Hybrid Composites for Automotive Applications - Development and Manufacture of a System-integrated Lightweight floor Structure in multi-material Design. In *Reinforcement Technologies*, Novi, MI, USA. DOI=10.24406/PUBLICA-FHG-405892.
- [19] McLeod, M., Héту, J.-F., Deaville, T., Bureau, M., and Baril, E. 2010. Morphological and Mechanical Comparison of Injection and Compression Moulding In-Line Compounding of Direct Long Fibre Thermoplastics. In *Advances in Thermoplastic Composites*, 109–119.
- [20] Osswald, T. A. Fiber Orientation and Warpage Prediction of DLFT/Thermoplastic Fiber Mats Hybrid Parts. Simulation and Experimental Validation.
- [21] Perez, C., Osswald, T., and Goris, S. 2013. Study on the fiber properties of a LFT strand. *SPE ACCE*, 1115–1126.
- [22] Peter Eyerer, W.Krause, F.Henning, S.Tröster, and O.Geiger. 2002. LFT-D – A Process Technology for Large Scale Production of Fiber Reinforced Thermoplastic Components. *Journal of Thermoplastic Composite Materials* 14.
- [23] Radtke, A. 2008. *Steifigkeitsberechnung von diskontinuierlich faserverstärkten Thermoplasten auf der Basis von Faserorientierungs- und Faserlängenverteilungen.* Wissenschaftliche Schriftenreihe des Fraunhofer ICT 45. Fraunhofer-IRB-Verl., Stuttgart, Germany.
- [24] Rohan, K., McDonough, T. J., Ugresic, V., Potyra, E., and Henning, F. 2014. Mechanical study of direct long fiber thermoplastic carbon/polyamide 6 and its relations to processing parameters. *SPE Automotive.*
- [25] Rohde-Tibitzl, M. 2015. *Direct Processing of Long Fiber Reinforced Thermoplastic Composites and their Mechanical Behavior under Static and Dynamic Load.* Hanser Publications, Cincinnati, OH, USA.
- [26] Schelleis, C., Scheuring, B. M., Liebig, W. V., Hrymak, A. N., and Henning, F. 2023. Approaching Polycarbonate as an LFT-D Material: Processing and Mechanical Properties. *Polymers* 15, 9, 2041.
- [27] Thomason, J. L. 2002. The influence of fibre length and concentration on the properties of glass fibre reinforced polypropylene: 5. Injection moulded long and short fibre PP. *Composites Part A: Applied Science and Manufacturing* 33, 12, 1641–1652.
- [28] Thomason, J. L. 2005. The influence of fibre length and concentration on the properties of glass fibre reinforced polypropylene. 6. The properties of injection moulded long fibre PP at high fibre content. *Composites Part A: Applied Science and Manufacturing* 36, 7, 995–1003.
- [29] Thomason, J. L. 2006. Structure-property relationships in glass-reinforced polyamide, part 1: The effects of fiber content. *Polym Compos* 27, 5, 552–562.
- [30] Thomason, J. L. 2007. Structure–property relationships in glass reinforced polyamide, part 2: The effects of average fiber diameter and diameter distribution. *Polymer Composites* 28, 3, 331–343.
- [31] Thomason, J. L. and Groenewoud, W. M. 1996. The influence of fibre length and concentration on the properties of glass fibre reinforced polypropylene: 2. Thermal properties. *Composites Part A: Applied Science and Manufacturing* 27, 7, 555–565.
- [32] Thomason, J. L. and Vlug, M. A. 1996. Influence of fibre length and concentration on the properties of glass fibre-reinforced polypropylene: 1. Tensile and flexural modulus. *Composites Part A: Applied Science and Manufacturing* 27, 6, 477–484.
- [33] Thomason, J. L. and Vlug, M. A. 1997. Influence of fibre length and concentration on the properties of glass fibre-reinforced polypropylene: 4. Impact properties. *Composites Part A: Applied Science and Manufacturing* 28, 3, 277–288.

- [34] Tröster, S. 2004. *Materialentwicklung und -charakterisierung für thermoplastische Faserverbundwerkstoffe im Direktverfahren*. Wissenschaftliche Schriftenreihe des Fraunhofer ICT Bd. 39. Fraunhofer-IRB-Verl., Stuttgart, Germany.
- [35] Truckenmüller, F. 1996. *Direktverarbeitung von Endlosfasern auf Spritzgießmaschinen. Möglichkeiten und Grenzen*. Zugl.: Stuttgart, Univ., Diss., 1996. Fortschritt-Berichte VDI Reihe 3, Verfahrenstechnik 444. VDI-Verl., Düsseldorf.
- [36] Truckenmüller, F. and Fritz H.-G. 1991. Injection molding of long fiber-reinforced thermoplastics: A comparison of extruded and pultruded materials with direct addition of roving strands. *Polymer Engineering & Science* 31, 18, 1316–1329.
- [37] Whitfield, T., Kuboki, T., Wood, J., Ugresic, V., Sathyanarayana, S., and Dagnon, K. 2018. Thermal properties of glass fiber reinforced polyamide 6 composites throughout the direct long-fiber reinforced thermoplastic process. *Polym Eng Sci* 58, 1, 46–54.